

Investigating fractal dimension, heart rate variability, and memory during different image sequencing regimes in young adults

Cite as: Chaos 30, 113116 (2020); <https://doi.org/10.1063/5.0002764>

Submitted: 30 January 2020 . Accepted: 19 October 2020 . Published Online: 06 November 2020

David Aguiard,  Vanessa Zarubin, Caroline Wilson,  Katherine R. Mickley Steinmetz, and  Carolyn Martsberger



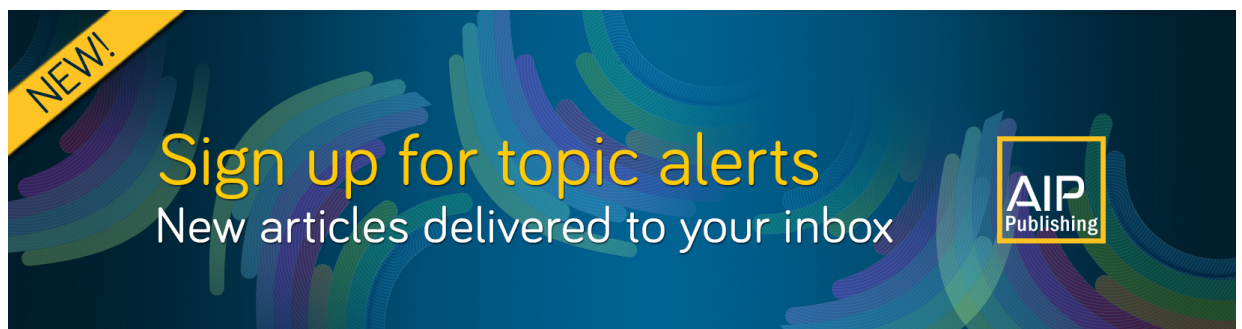
View Online



Export Citation



CrossMark



NEW!

Sign up for topic alerts

New articles delivered to your inbox

AIP Publishing



Investigating fractal dimension, heart rate variability, and memory during different image sequencing regimes in young adults

Cite as: Chaos 30, 113116 (2020); doi: 10.1063/5.0002764

Submitted: 30 January 2020 · Accepted: 19 October 2020 ·

Published Online: 6 November 2020






View Online



Export Citation



CrossMark

David Aguillard,¹ Vanessa Zarubin,²  Caroline Wilson,¹ Katherine R. Mickley Steinmetz,²  and Carolyn Martsberger^{1,a)} 

AFFILIATIONS

¹Department of Physics, Wofford College, 429 N Church Street, Spartanburg, South Carolina 29303, USA

²Department of Psychology, Wofford College, 429 N Church Street, Spartanburg, South Carolina 29303, USA

^{a)}Author to whom correspondence should be addressed: martsbergercm@wofford.edu

ABSTRACT

The goal of this study is to investigate patterns that emerge in brain and heart signals in response to external stimulating image regimes. Data were collected from 84 subjects of ages 18–22. Subjects viewed a series of both neutrally and negatively arousing pictures during 2-min and 18-s-long segments repeated nine times. Both brain [electroencephalogram (EEG)] and heart signals [electrocardiogram (EKG)] were recorded for the duration of the study (ranging from 1.5 to 2.5 h) and analyzed using nonlinear techniques. Specifically, the fractal dimension was computed from the EEG to determine how this voltage trace is related to the image sequencing. Our results showed that subjects visually stimulated by a series of mixed images (a randomized set of neutrally or negatively arousing images) had a significantly higher fractal dimension compared to subjects visually triggered by pure images (an organized set of either all neutral or all negatively arousing images). In addition, our results showed that subjects who performed better on memory recall had a higher fractal dimension computed from the EEG. Analysis of EKG also showed greater heart rate variability in subjects who viewed a series of mixed images compared to subjects visually triggered by pure images. Overall, our results show that the healthy brain and heart are responsive to environmental stimuli that promote adaptability, flexibility, and agility.

Published under license by AIP Publishing. <https://doi.org/10.1063/5.0002764>

In this study, we capture simultaneous brain and heart data in healthy subjects to investigate the connection between the underlying nonlinear nature of voltage patterns to external image regimes. For example, we found differences in the fractal dimension (FD) of the electroencephalogram (EEG) when subjects were visually stimulated by a series of categorized pictures. Specifically, subjects visually stimulated by a series of mixed images (a randomized set of neutrally or negatively arousing images) had a significantly higher fractal dimension compared to subjects visually stimulated by pure images (an organized set of either all neutral or all negatively arousing images). Analysis of electrocardiogram (EKG) also showed greater heart rate variability (HRV) in subjects who viewed a series of mixed images compared to subjects visually triggered by pure images. In addition to these results, we found that subjects who had better memory recall had significantly higher fractal dimensions. These results may have medical implications in terms of how we might non-invasively investigate

memory and physiological fitness. This is also an important result to highlight the ubiquity of physics techniques in a variety of relevant fields.

INTRODUCTION

Scientists across fields have computed the fractal dimension (FD) of signals in a variety of systems in order to more fully understand how nonlinearity plays a significant role in system behavior (Goldberger and West, 1987; Katz, 1988; Kesic and Spasic, 2016; Stam, 2005; and Wright *et al.*, 1993). FD measures the degree of nontrivial self-similarity in a system, the persistence of patterns, or characteristic features of the system's morphology over multiple scales (Captur *et al.*, 2017; Nayyeri, 2017; and Riley *et al.*, 2012). In other words, FD quantifies the characteristic patterns viewed on a large scale that repeat on smaller scales

(Arsac and Deschodt-Arsac, 2018). The fractal behavior of a system, classified by neither exclusively regular nor entirely random fluctuations, has been shown to be correlated with better health outcomes (Iyengar *et al.*, 1996). In many cases, the level of fractal scaling can be used to differentiate between healthy and pathological subjects (Golinska, 2012). Studies have reported that decreased complexity or altered fractal dimensions reflect impaired adaptive response to physiological stress as a result of aging or disease (Arsac and Deschodt-Arsac, 2018; Golinska 2012; Iyengar *et al.*, 1996; and Peng *et al.*, 1995). Typically, we associate irregular, complex signals with normal physiology, while consistent patterns are indicative of reduced function (Pincus and Goldberger, 1994). Furthermore, subjects with improved clinical outcomes display a certain range of fractal behaviors, which are considered a signature of nonlinearity (Delignieres *et al.*, 2006). These patterns are visible on both long and short time scales and suggest a degree of complexity that may be indicative of human health; visualization and analysis of these physiological signals could play a role in predicting and recognizing a disease (Nayyeri, 2017 and Pincus and Goldberger, 1994). By looking at the FDs in EEG data in this study, we aim to obtain information from standard voltage traces about their complexity under different external image regimes and in relation to a subject's overall memory capabilities.

In addition to FD, we investigate the influence of these external image regimes on heart rate variability in EKG data. Short-term heart rate variability is evident and quantifiable by numerous methods (Piskorski and Guzik, 2007). Studies have shown that decreases in heart rate variability may accompany adverse health states (Pincus and Goldberger, 1994), and healthy heart dynamics often demonstrate high frequency heart rate fluctuations (Iyengar *et al.*, 1996). These beat-to-beat fluctuations shown in the healthy heart may be related to properties of cardiac and neural systems controlling their output (Peng *et al.*, 1995). Because low heart rate variability has been associated with compromised health, while greater fluctuations have been linked to normal, healthy physiology, the study of fluctuations in the heart rate holds promising information for clinical and predictive measures (Captur *et al.*, 2017; Pincus and Goldberger, 1994; and Shaffer and Ginsberg, 2017). Our work seeks to quantify changes in the EKG to explore the connections between signal characteristics and performance as an indicator of health.

In this study, we use mathematical techniques such as fractal dimension for the brain (EEG) signals and heart rate variability metrics for the heart (EKG) signals to calculate the degree of complexity, self-similarity, and variability of voltage signals acquired. We find FD in the brain and short-term heart rate variability metrics in the heart to investigate how these parameters correlate with visual stimuli and a subject's recall capability. We hypothesize that highly complex signals in the brain and greater variability of signals in the heart may be correlated with the external image regime and indicative of better overall performance on memory recall.

METHOD

Participants

84 undergraduate students from the Wofford College (58 female) between the ages of 18 and 22 ($M = 19.98$, $SE = 0.125$) participated in this study for either course credit or a \$20 Amazon

gift card. All participants provided written informed consent, and procedures were approved by the Wofford College Institutional Review Board. Six participants were excluded from analysis on the basis of prior exposure to the images ($n = 2$), left-handedness ($n = 1$), connection failure ($n = 1$), and neurological disorder ($n = 2$). An additional 11 participants were excluded from the analysis due to poor signal capture. Three more participants were omitted from the heart rate analysis due to a low-quality EKG. This resulted in a sample of 67 participants (47 female) included in the brain analyses and 64 participants (44 female) included in the heart analyses. All participants were right-handed. Each participant was assigned to either a pure image regime ($n = 32$ for the brain; $n = 31$ for the heart) or a mixed image regime ($n = 35$ for the brain; $n = 33$ for the heart). Pure and mixed image regimes are described below. Participants were not currently abusing drugs, did not receive general anesthesia in the two weeks prior to testing, and did not sustain a concussion in the month prior to testing.

Study materials: Image regimes explained

In this study, two image regimes (pure and mixed) were created for subjects to view. To create these two image regimes, the following protocol was implemented. 66 negative, 66 related neutral (we will refer to as categorical), and 66 unrelated neutral (we will refer to as neutral) images resized to 500 by 400 pixels were selected from a pool of 100 unrelated neutral images, 150 related neutral images, and 150 negative images sourced from the International Affective Picture System (Lang *et al.*, 1995), the Geneva Affective Picture Database (Dan-Glauser and Scherer, 2011), the Emotional Picture Set (Wessa *et al.*, 2010), the image pool of Talmi *et al.* (2007), and Google Images. Participants rated images on arousal (perceived physiological state), valence (how pleasant or unpleasant the image made the participant feel), and relatedness (how semantically associated with other pictures a particular image was) in pilot studies. Participants rated both arousal and valence on nine-point scales. For arousal, the scale was graded from "calm/soothing" to "exciting/agitating." For valence, the scale ranged from "very displeasing" to "very pleasing." Participants rated images' relatedness on a seven-point scale from "low association" to "high association." Participants were given examples of categorically related images (a handgun and a rifle; walking and running) as well as thematically related images (an umbrella and clouds) prior to rating. To ensure that image categories did not differ in brightness or complexity, the luminosity rating was also calculated for each image using Photoshop, and complexity ratings were taken from three independent raters.

Subjects were randomly assigned to either a pure image regime or a mixed image regime. In the pure image regime, subjects viewed images that were all neutral, all negative, or all categorical for a total of nine segments. Each segment contained 22 images from one of the three groups (i.e., negative, neutral, or categorical). The nine segments were always ordered in the following way: negative (segment 1), categorical (segment 2), neutral (segment 3), categorical (segment 4), neutral (segment 5), negative (segment 6), neutral (segment 7), negative (segment 8), and categorical (segment 9). For the mixed image regime, subjects viewed nine segments of a mix of neutral, negative, and categorical images for every segment. For example, in the mixed list for segment 1, the 22 images were

TABLE I. Means and standard errors for pure image selections.

	Negative mean	Negative standard error	Categorical mean	Categorical standard error	Neutral mean	Neutral standard error
Arousal	7.212	0.075	4.872	0.083	4.838	0.068
Valence	2.711	0.074	5.139	0.086	5.090	0.058
Relatedness	3.626	0.085	3.589	0.048	1.981	0.017
Luminosity	106.105	3.048	106.353	1.304	107.516	3.030
Complexity	3.025	0.085	3.062	0.116	3.025	0.134

a random sampling of negative, neutral, and categorical images. Overall, image regimes were balanced such that negative images were rated significantly lower on valence and significantly higher on arousal than either categorical or neutral, which did not significantly differ from each other on either measure (Tables I and II). Both negative and categorical images were rated as significantly more related than neutral images but did not differ from each other in relatedness (Tables I and II). All image types were matched on both complexity and luminosity (Tables I and II). An additional categorical list and an additional mixed list were created to be used as the practice test from unselected images rated in the initial pool. The practice test gave participants an opportunity to try the testing procedure before recordings started.

Participants reported their depression and anxiety levels using standardized questionnaires including a 19-item version of the Beck Depression Inventory (BDI-I; Beck *et al.*, 1961) and a 21-item version of the Beck Anxiety Inventory (BAI; Beck *et al.*, 1988), both of which have been demonstrated as reliable and concise measures of depression and anxiety levels.

Procedure

After participants gave consent to participate in the study, a Cortech ActiveTwo 32 Channel EEG System (Manufacturer: Cortech Solutions; Model Specifications: Model Number DA-AT_HCL32) from the Behavioral Brain Sciences Center, Birmingham, UK, was applied to the participant's scalp while he or she completed the depression and anxiety questionnaires (BDI-I and BAI) and the practice test.

The experiment consisted of nine segments. In each segment, participants first viewed 22 images. Images were presented in

TABLE II. t-test image-balancing comparisons between selected image pools. Significant differences denoted by <0.001 . As intended, negative images were more arousing and negatively valenced than either neutral groups but did not differ in luminosity or complexity. In addition, negative and categorical images were more related than neutral images.

	Neutral to categorical	Negative to neutral	Negative to categorical
Arousal	0.752	<0.001	<0.001
Valence	0.634	<0.001	<0.001
Relatedness	<0.001	<0.001	0.706
Luminosity	0.724	0.743	0.940
Complexity	0.838	0.999	0.801

E-Prime 3.0 (Psychology Software Tools, Pittsburgh, PA). Each image was presented for 2 s followed by a fixation cross (solid white screen with a central black plus sign symbol) that was presented for 4 s. The fixation cross between each image was used to reduce any remaining emotional responses carrying over from the previous image (Talmi and McGarry, 2012). After viewing all 22 images, participants completed a 1-min arithmetic task, which prevented them from having an increased memory for the images that appeared at the end of the list. Following the arithmetic task, participants were asked to recall as many images as they could for up to 3 min.

Data processing and reduction

For the EEG recording, sites were referenced online to two mastoid electrodes and re-referenced offline using the common average reference. Electrode offsets were between 0 and ± 30 mV. Signals were amplified, bandpass filtered (0.03–30 Hz), and digitized at 1024 Hz. Two EOG electrodes were used to track eye movements. Three EKG electrodes also recorded heart rate data during the experiment. All data were cleaned to remove any artifacts that impeded the voltage signals. Blinks were removed using the Electromagnetic Source Estimation (EMSE) manual artifact tool.

Analyses were performed based on image regimes (pure vs mixed). Fractal dimensions were computed in EEG, and heart rate variability metrics were computed in EKG to determine the impact of the two image lists (pure vs mixed) on the acquired signals. Complexity in EEG and variability in the heart were also analyzed in connection with overall memory performance. To investigate EEG and EKG patterns from subjects who viewed the mixed image regime vs the pure image regime, we ran a standard independent sample t-test in SPSS Statistics software to compare the mean from these two groups. All reports used Levene's Test for Equality of Variances (with equal variances not assumed) to determine p-value statistics. We also computed paired sample t-tests within each subject during testing to analyze drift and variation throughout the course of the study. Furthermore, we looked at the difference in each image regime to see if patterns emerged within each list type (i.e., analysis entirely within the pure image regime). We also computed fractal dimensions and heart rate variability in correlation with subjects' memory scores (MSs). The level of significance was set at $p = 0.05$, although in some cases, marginal significance of $0.05 < p < 0.06$ is noted.

Analyzing voltage data

Data were analyzed using robust methods to determine self-similarity and variability. Voltage signals acquired from the

scalp (i.e., EEG signals) were analyzed using the Higuchi method to determine FD (Higuchi, 1988). Data acquired from the EKG were analyzed using short-term heart rate metrics. These were obtained by analyzing the time between two consecutive R-waves of the EKG known as the RR interval. We used the RR interval to determine the percentage of sequential RR intervals that differ by more than 50 ms (pNN50), the standard deviation (SD) of the Poincaré plot perpendicular to the line of identity (SD1) and along the line of identity (SD2) and the standard deviation of normal to normal intervals (SDNN) (Shaffer and Ginsberg, 2017). The results are discussed below.

Computational methods for the brain

The Higuchi method was used to determine a metric of complexity for the brain. This method of calculating fractal dimensions determines the length of the curve for a collection of a time series. The time series is defined as $X_k^m; X(m), X(m+k), X(m+2k), \dots, X(m + \frac{N-m}{k} \cdot k)$, ($m = 1, 2, \dots, k$), in which m and k are integers representing the initial time and the interval time, respectively, and N represents the total number of data points. The length of the curve X_k^m is then given by

$$L_m(k) = \left\{ \left[\sum_{i=1}^{\left\lfloor \frac{N-m}{k} \right\rfloor} |X(m+ik) - X(m+(i-1) \cdot k)| \right]^{\frac{N-1}{N-m \cdot k}} \right\} / k.$$

For the time interval k , the curve length $\langle L(k) \rangle$ represents the average value over k sets of $L_m(k)$. A value for $\langle L(k) \rangle$ proportionate to k^{-D} indicates a fractal with dimension D (Higuchi, 1988).

In order to use the Higuchi algorithm to calculate FD, we needed to determine a maximum value for the algorithm's dependent parameter k , which we define as K_{max} . The parameter k refers to the time interval between time series observations and represents the number of distinct sets of time series obtained from various initial times. The model was optimized via a computational experiment to determine a K_{max} value that would be used for all electrodes. In order to determine K_{max} , six electrodes were chosen from equally spaced regions within the electrode grid to give the best visual of the expanse of the brain. Specifically, electrodes Fp1, T7, Oz, T8, Fp2, and Cz were chosen from the brain (see Fig. 1). Data from these six electrodes were used to determine the optimal K_{max} to run the Higuchi algorithm so that the fractal dimension plateaued and the computational run time was reasonable. A K_{max} of 58 was determined to be the optimal value to achieve both goals. To confirm this result, we also computed the peak of the sum of differences of the fractal dimension as a function of K_{max} (from 1 to 100) in every subject for the six chosen electrodes. Five out of six electrodes had their peak at $K_{max} = 58$.

After determining a K_{max} value of 58 computationally, we divided the raw EEG from all 32 electrodes of each participant into nine segments, which corresponded to the nine periods when the subject viewed the images. Each segment lasted 2 min and 18 s and includes data from 3 s before the subject viewed the first image until 2 s after the subject viewed the final image. The nine segments of EEG data were then run through the Higuchi algorithm for each of the 32 electrodes individually so that every participant had 32 FD values associated with each segment, one value for each electrode on the cap. The arithmetic mean of the 32 FD values was also computed

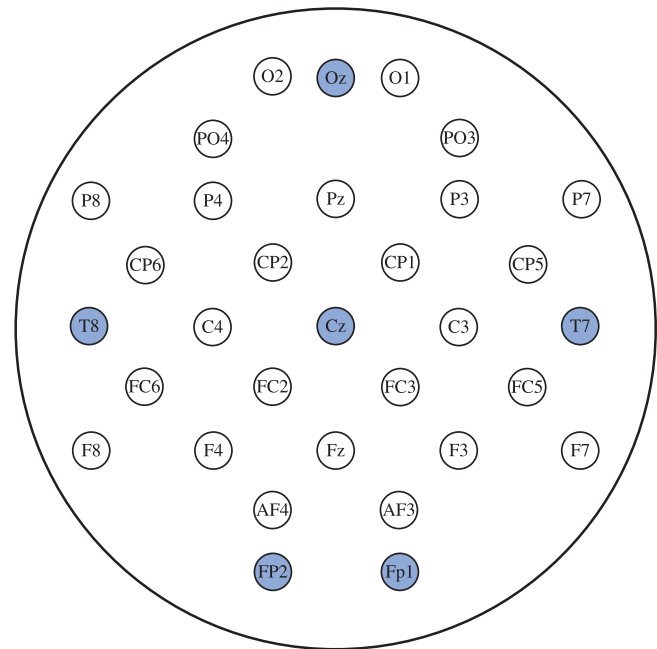


FIG. 1. Map of 32 electrodes highlighting the 6 electrodes from which K_{max} was computed.

to find the average fractal dimension (AFD) per participant for each segment.

To assign a memory score, we analyzed each subject's performance in memory after each segment by asking participants to describe every image they could remember from that segment. The memory score was measured by the percentage of images in each group correctly identified as remembered. Subjects were also given three separate scores from 0 to 100 for their ability to recall negative, neutral, and categorical images. The subjects' recall was highest on negative images, which is consistent with the literature (Talmi *et al.*, 2007; Kensinger, 2009; Talmi and McGarry, 2012; and Schmidt and Saari, 2007).

In addition to calculating FDs for each of the nine individual segments, for participants who viewed pure lists that were only categorical, negative, or neutral for the entire duration of each segment, we also computed the average FD and the FDs of the 32 electrodes across the three categorical, three neutral, and three negative segments to analyze each segment type (i.e., negative, neutral, and categorical). This gave us a single AFD and an electrode-based fractal dimension associated with each of the image types (negative, neutral, and categorical) for each participant viewing the pure image regime. We compared the calculated FD values of each image type (negative, neutral, and categorical) to corresponding memory scores for each image type. Similarly, for each of the mixed image regimes, we computed the AFD and each electrode's FD across the nine individual segments as well as across the triplet of segment type to evaluate FD values in relation to memory scores and in comparison with the corresponding pure segment types.

Analyzing the heart rate data

The participants' EKG data recorded during each of the nine segments were split into 6-s intervals. Each 6-s interval commenced when the subject began viewing a given image and ended before the following image was shown. These segments were normalized and filtered through MATLAB's Savitzky-Golay filter (Sgoley, MathWorks).

We used MATLAB's "findpeaks" algorithm to identify each R wave peak to extract RR interval data. After initial cleaning, the 6-s segments were stitched back together, and two independent research assistants manually checked the data for false and missed RR interval assignments. These were corrected manually before the voltage data were analyzed.

RR intervals were analyzed for SDNN, pNN50, SD1, and SD2. The standard deviation of normal-to-normal intervals (SDNN) (normal referring to heartbeats originating only in the sinoatrial node rather than being induced ectopically, or elsewhere) and the percentage of successive RR intervals that differ by more than 50 ms (pNN50) are measurements that seek to quantitatively address the variability present in time intervals between heartbeats. SD1 and SD2 are nonlinear measures of heart rate variability that apply standard deviations of points from the Poincaré scatterplot to visualize patterns and trends of time series.

FINDINGS AND ANALYSIS

Brain results: Fractal dimension in EEG and image regimes

Fractal dimensions were computed for each electrode (32 total) from the expanse of the brain. We also report the fractal dimension averages from all 32 electrodes (AFD). Fractal dimensions are presented for each segment type (negative, neutral, and categorical), over the entire nine segments, and segment-by-segment (i.e., 1–9).

Subjects viewing mixed image regimes had overall higher FDs when compared to the FDs of subjects who viewed pure image regimes. We created brain maps to identify the electrodes that exhibited significant behavior between the mixed image regime and the pure image regime. The brain maps are presented in Fig. 2. Specifically, the fractal dimensions were higher ($p < 0.05$) in subjects viewing the mixed vs the pure lists. For example, for the entire set of all nine segments, 16 of the 32 electrodes displayed significance as highlighted in Fig. 2(a). This result persisted for the average computed over segment types. To calculate the averages over the segment type, we implemented the following procedure. First, we averaged the FD per electrode of all three neutral segments (pure segments 3, 5, and 7) from the pure subjects and compared the result to the FD averages of the corresponding mixed list segment numbers (mixed segments 3, 5, and 7) of the mixed subjects. We found that 20 out of 32 electrodes had a statistically significant higher FD for the mixed list compared to the pure neutral list [Fig. 2(b)]. Similarly, comparing the three categorical segments (pure segments 2, 4, and 9) from the pure subjects to the corresponding mixed list segment numbers (mixed segments 2, 4, and 9) reveals that 14 out of 32 electrodes were significant during the categorical segments [Fig. 2(c)]. Finally, comparing the three negative segments (pure segments 1, 6, and 8) to the corresponding mixed list segments (mixed segments

1, 6, and 8), we found that 10 out of 32 electrodes were significant [Fig. 2(d)]. In each of the cases reported, fractal dimensions were higher in subjects stimulated by mixed image lists as opposed to image lists organized according to the image type (categorical, negative, or neutral). The AFD for this result is reported in Fig. 3. Overall, higher FD corresponded to the mixed image regime. Since subjects who viewed the mixed image regime had an overall higher FD compared to subjects who viewed the pure image regime, we hypothesize that an alternating external image regime may influence EEG. These data may suggest that mixing images that evoke a range of emotional responses caused a constant switching in the brain that contributed to a more complex waveform, whereas the methodical nature of the pure lists reduced the complexity of the corresponding brain signals, possibly due to habituation of the type of image the subject viewed throughout the sequence. A mixed image regime seems to illicit a more malleable, dynamic response in subjects compared to the consistent sequence resulting from the pure regime.

Fractal dimension based on segment number (i.e., 1–9) was also computed as a function of the pure or mixed image regime. Specifically, the fractal dimension was averaged over all electrodes per subject during each of the nine segments. The average fractal dimension per segment was compared between image regimes (mixed and pure). In comparing each of the segments between the pure and mixed subject assignments, six out of nine segments were statistically significant (Fig. 4). In particular, FD values from the mixed group were significantly higher in the first six segments of testing (i.e., the first sequential two-thirds of the testing period) corresponding to the negative, categorical, neutral, categorical, neutral, and negative segments. The last three segments (neutral, negative, and categorical) did not exhibit significance in FD. Comparing the pure vs the mixed groups reveals that participants who viewed mixed lists had a statistically significant higher fractal dimension compared to the subjects who viewed pure lists (categorical, negative, or neutral) during the first six segments of testing. This is consistent with our first reported finding that the mixed image regime showed significantly higher FDs than the pure image regime.

In summary, subjects stimulated by mixed image lists had higher FDs when compared to subjects stimulated by pure image lists organized according to image type (categorical, negative, or neutral). This suggests that the FD may be influenced by a visually changing external image regime, and variable external patterns of stimulation contribute to activating the brain differently compared to an external image regime in which the same thematic group of images occurs. This may suggest that an alternating image regime can evoke a different response in the resulting voltage pattern compared to a constant image regime, which may be applicable to developing a form of clinical stress testing to investigate brain fitness or to crafting a therapeutic exercise, based on a switching stimulus pattern.

Brain results: Fractal dimension in EEG and memory

Our finding that the fractal dimensions were higher in the mixed list case vs the pure list case suggests that the image regime pattern evoked a response in subjects who scaled with complexity. We also investigated the fractal dimension of subjects with their respective memory scores in a similar manner. We found

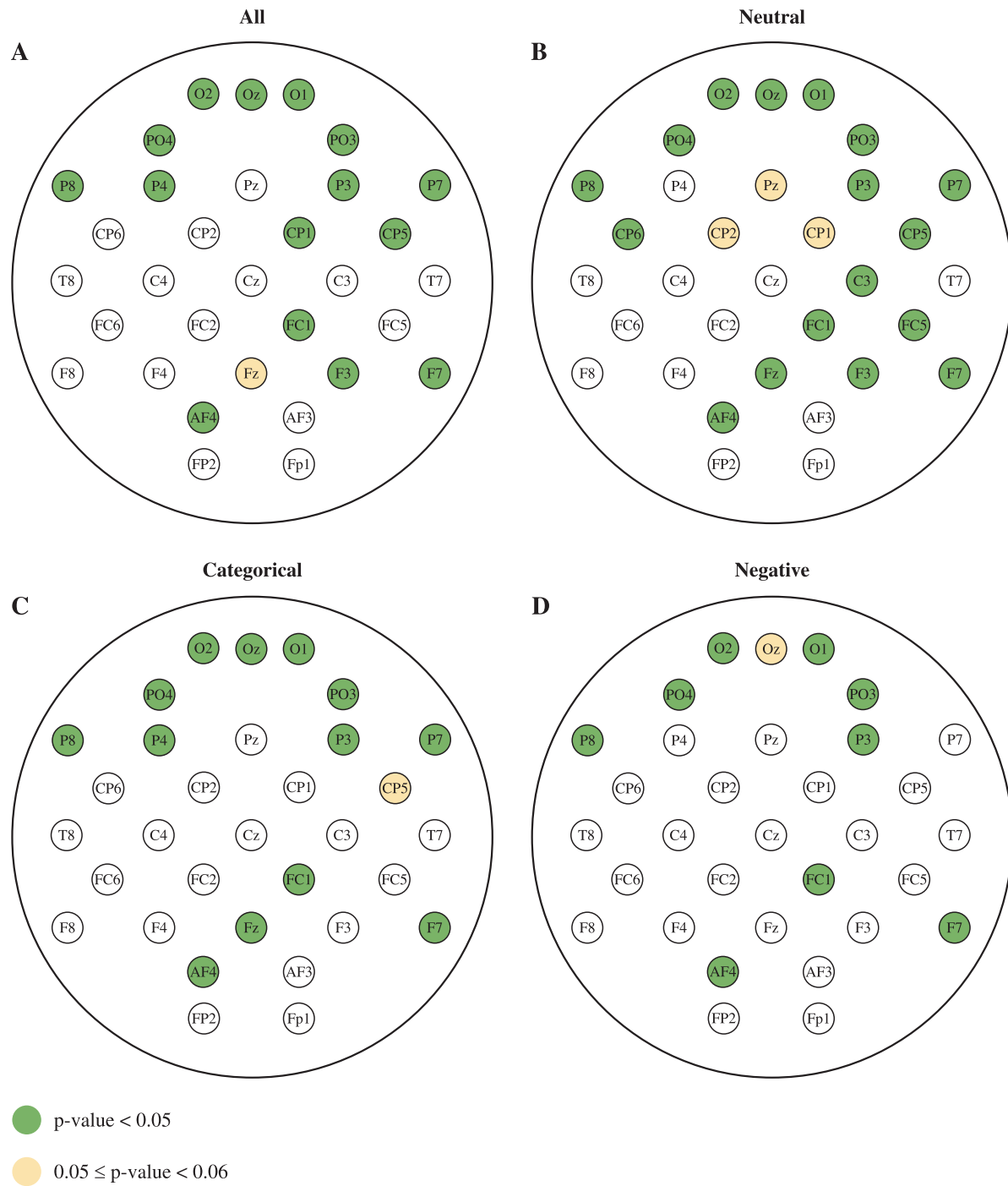


FIG. 2. Electrode maps illustrating significant fractal dimensions for different segment types and all segments. Highlighted electrodes in (a) illustrates the location of electrodes with higher FD for the mixed image regime compared to the pure image regime for all segments. (b) shows the electrodes with higher FD for the mixed image regime compared to the pure image regime for neutral segments. (c) shows the electrodes with higher FD for the mixed image regime compared to the pure image regime for categorical segments. (d) shows the electrodes with higher FD for the mixed image regime compared to the pure image regime for the negative segments.

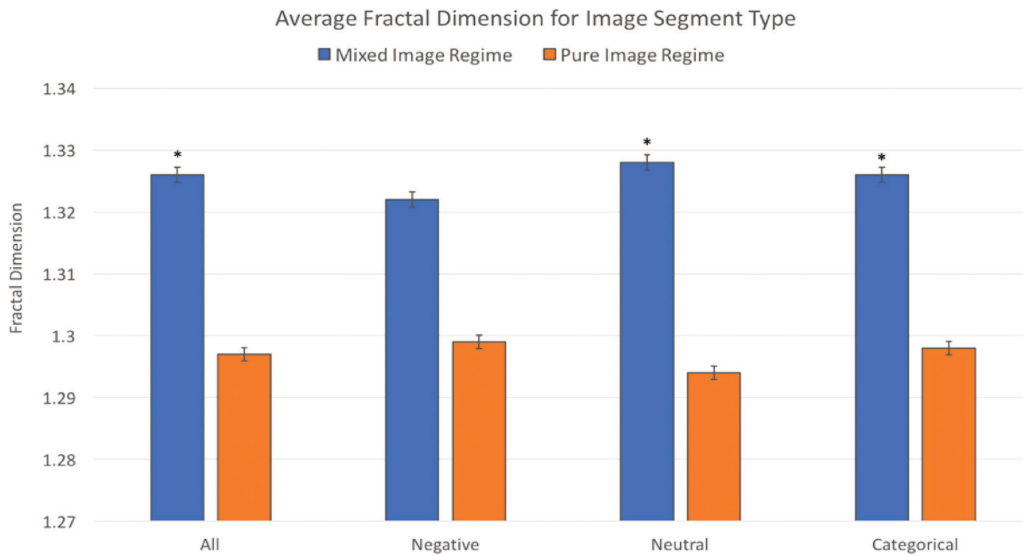


FIG. 3. Average fractal dimension (AFD) for the mixed image regime (blue) and the pure image regime (orange). Results are presented for the segment types [negative (p-value = 0.079), neutral (p-value = 0.007), and categorical (p-value = 0.027)] as well as for all segments [all (p-value = 0.024)]. Our results show that the mixed image regime has a significantly higher FD (denoted by *) compared to the pure image regime.

that for subjects viewing pure images only, there was a correlation between their memory score and their fractal dimensions. Specifically, subjects who had higher memory scores also had higher fractal dimensions. We found this result under the following conditions. For subjects who viewed negative images, a higher memory score correlated with higher fractal dimensions in 21 of the 32 electrodes (with 5 of the 21 electrodes displaying marginal significance). We illustrate this finding in the brain map [Fig. 5(a)] and in Fig. 6 for

the AFD. Similar results for the categorical data showed a correlation between higher fractal dimensions and higher memory score in 18 out of the 32 electrodes, displayed in Figs. 5(b) and 6 for the AFD. This supports findings emphasizing the role of semantic relatedness in memory processes, favoring categorical stimuli over random (Talmi and Moscovitch, 2004). For the case of neutral segments, we found that 4 out of the 32 electrodes were significant. This finding is illustrated in Figs. 5(c) and 6 for the AFD. Overall, these data suggest

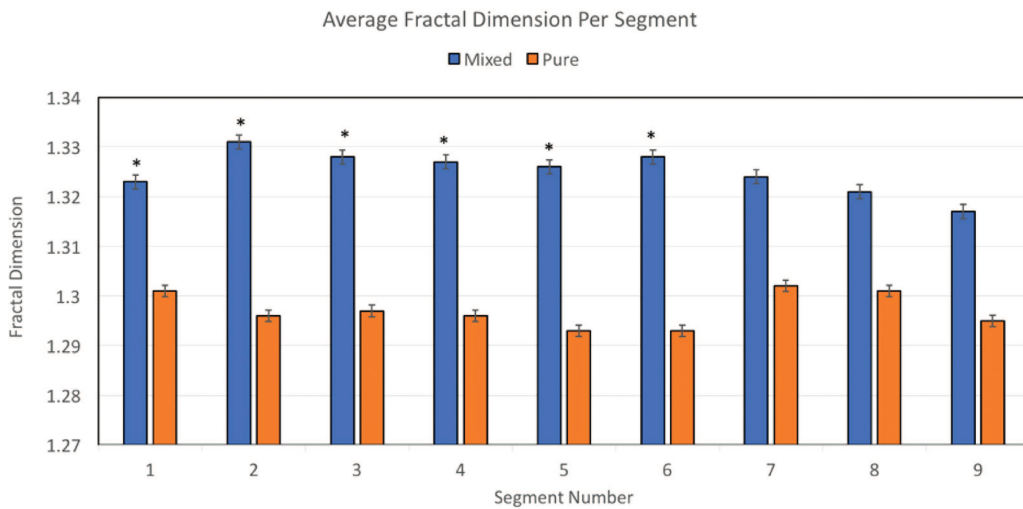


FIG. 4. Average fractal dimension (AFD) per segment for the mixed image regime (blue) and the pure image regime (orange). Our results show that the mixed image regime has significantly higher FDs (denoted with *) for the first six segments compared to the pure image regime.

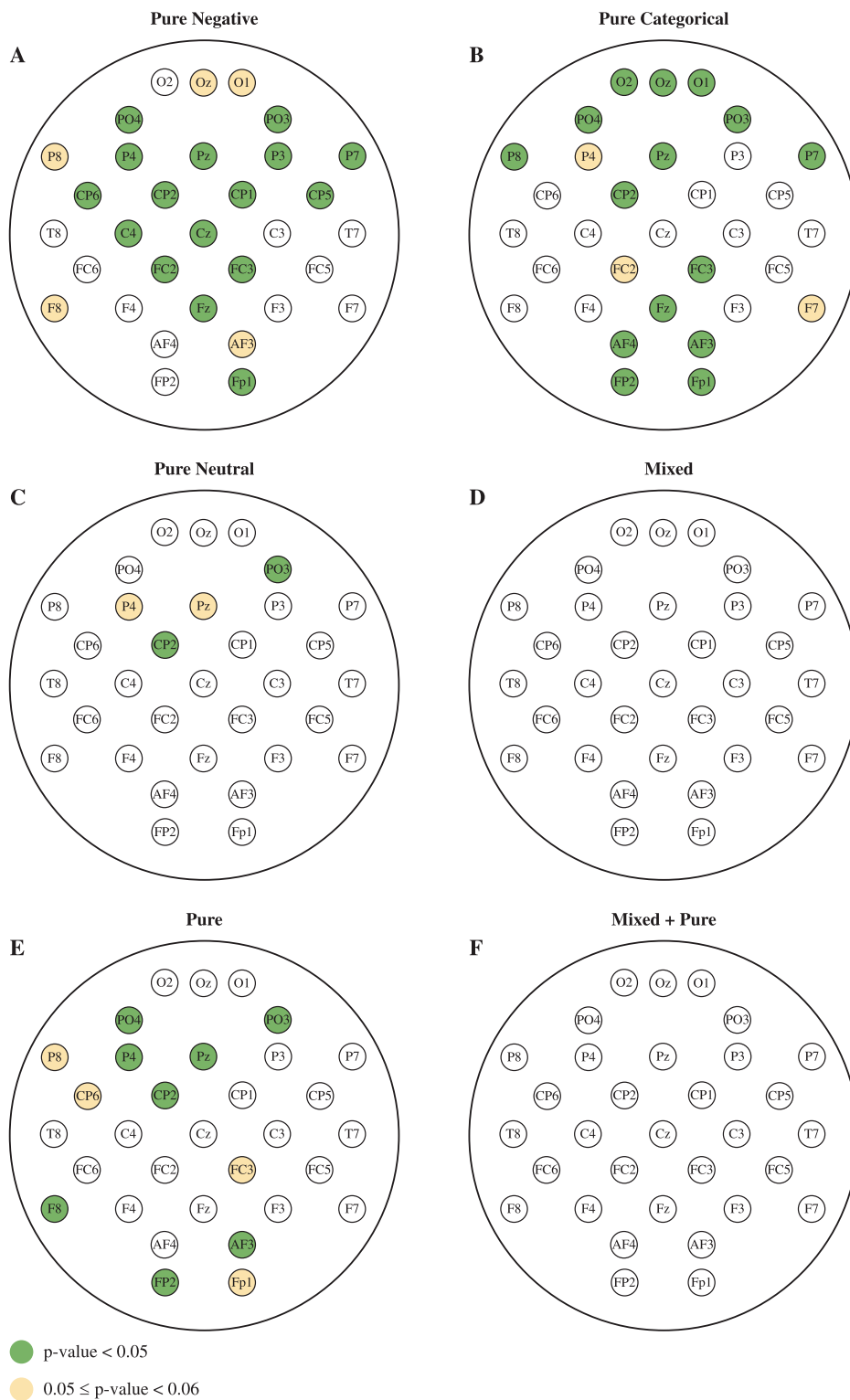


FIG. 5. Electrode maps illustrating fractal dimensions by memory. Higher fractal dimensions were correlated with better memory scores in highlighted electrodes. (a) illustrates higher fractal dimension with better memory scores for subjects viewing the negative pure image regime. (b) illustrates higher fractal dimension with better memory scores for subjects viewing the categorical pure image regime. (c) illustrates higher fractal dimension with better memory scores for subjects viewing the neutral pure image regime. (d) illustrates that there was no correlation between FD and better memory for the subjects who viewed the mixed image regime. (e) illustrates that there was a correlation between FD and better memory for the subjects who viewed all nine segments of the pure image regime. (f) illustrates that there was no correlation between FD and better memory for all subjects viewing the mixed or pure image regimes.

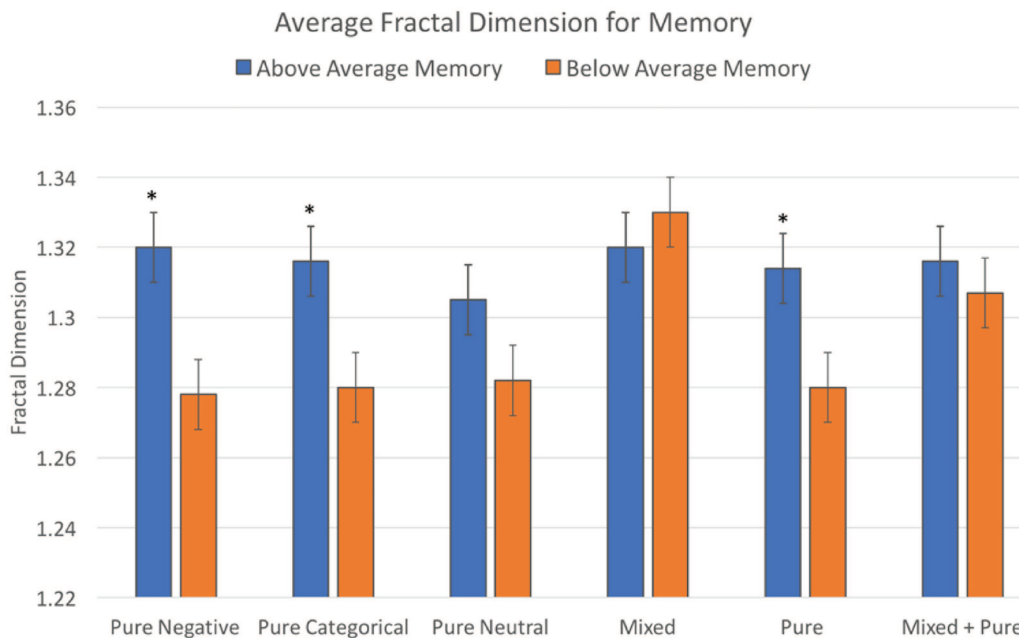


FIG. 6. Average fractal dimension vs memory. FD as it relates to memory during the pure image regime only is presented in the first three pure results [pure negative (p -value = 0.014), pure categorical (p -value = 0.023), and pure neutral (p -value = 0.172)]. Subjects in the pure image regime with above average memory had higher FDs. FD as it relates to memory for the entire pure regime only [pure (p -value = 0.040)], the entire mixed regime only [mixed (p -value = 0.602)], and the entire data set [mixed + pure (p -value = 0.521)] is also presented. * denotes significance.

that greater complexity of a subject's brain data is correlated with a positive memory outcome, which may provide a foundation for future research possibilities.

For subjects viewing entirely mixed lists, there was no correlation between memory and fractal dimensions. This result is illustrated in Figs. 5(d) and 6 for AFD. Similarly, the data over all pure and mixed segments together demonstrated no clear evidence that memory was correlated with fractal dimension [Figs. 5(f) and 6]. However, for subjects viewing entirely pure lists over all nine segments, we found that 12 out of the 32 electrodes had higher fractal dimensions as the memory score increased. This result is illustrated in Figs. 5(e) and 6 for the AFD. Because all pure segments, whether averaged over all nine segments [Fig. 5(e)] or binned either according to image type [Figs. 5(a)–5(c)], show a correlation between better memory scores and higher fractal dimensions, our findings suggest that heightened memory recall may be correlated with a more complex neurological voltage pattern. On the contrary, all mixed segments and all pure and mixed segments together do not show significance in fractal dimensions with memory, suggesting that the effect can be washed out by an experience that mitigates recall.

The result in this section is supported by our analysis of memory scores. Specifically, there was no significant difference in FDs between subjects in the mixed image regime compared to those in the pure image regime for their corresponding memory scores (MSs) [$MS(\text{mixed}) = 44.36$ vs $MS(\text{pure}) = 46.21$, $p = 0.542$]. Likewise, we do not find statistically different MSs when comparing within subjects based on list types [negative ($MS(\text{mixed}) = 52.04$

vs $MS(\text{pure}) = 55.36$, $p = 0.272$], neutral [$MS(\text{mixed}) = 35.28$ vs $MS(\text{pure}) = 37.76$, $p = 0.474$], and categorical [$MS(\text{mixed}) = 45.47$ vs $MS(\text{pure}) = 46.01$, $p = 0.884$]. Because there was no difference between memory scores of the mixed and pure lists, we would not expect to see correlation between fractal dimension and memory when we look at the results from subjects in the pure and mixed image regimes all together. Because the mixed regime-only analysis shows no correlation, it is likely that the mixed image regime results wash out the effects of the correlation between FD and memory because the mixed image regime promotes memory recall differently than the pure image regime. Previous studies support that recall is diminished for neutral items in mixed compared to pure lists (Watts *et al.*, 2014 and Barnacle *et al.*, 2018). However, for our study, within subjects exposed to the pure image regime only, there is statistical significance ($p < 0.000001$) in MS for all inter-segment type matches (neutral vs negative, negative vs categorical, and categorical vs neutral), with the following MS values: $MS(\text{negative}) = 55.36$, $MS(\text{category}) = 46.01$, and $MS(\text{neutral}) = 37.77$. This result suggests that subjects remember negative images best, followed by categorical images and then neutral images. This finding is confirmed by other studies (Talmi and McGarry, 2012 and Talmi, 2013). Viewing the corresponding FD brain maps in Fig. 5, this result is reaffirmed in our findings of fractal dimensions. For Fig. 5(a), the negative segments that correspond to the highest memory recall in subjects also correspond to the largest number of electrodes (21 electrodes) that are significant in the correlation between memory and fractal dimension. The categorical segments also illustrate this correlation

but not in as many electrodes (18 electrodes) [Fig. 5(b)], and these segments correlate with the mid-range memory scores from subjects. Finally, the neutral segments illustrate the least number of electrodes (four electrodes) that show correlation with memory and fractal dimensions [Fig. 5(c)], which is consistent with the fact that they also represent the set of images with the lowest memory recall in subjects. Overall, the data suggest that higher memory scores during the pure image regime are related to higher fractal dimensions, which may have implications for the connection between brain complexity and overall memory capabilities.

To protect from family wise errors when making multiple hypotheses, results were presented for the entire cohort (represented above as the AFD). In addition, results from a Bonferroni correction are listed below for the 32 electrode cap, segment type, and segment number results. For the 32-electrode cap for the pure vs mixed image regimes, electrodes P7, PO3, and P8 had a p -value $< 1.5625 \times 10^{-3}$ (P7 p -value = 5.9023×10^{-4} , PO3 p -value = 1.52739×10^{-3} , and P8 p -value = 1.34024×10^{-3}). Similarly, for the 32-electrode cap for the above average memory vs the below average memory pure negative group, electrodes CP5, PO3, and Pz had a p -value $< 1.5625 \times 10^{-3}$. For the results of pure vs mixed image regimes on segment number, segment 2 had a p -value $< 5.55556 \times 10^{-3}$. For the pure vs mixed based on the segment type, the pure neutral vs mixed had a p -value of 0.007, satisfying the Bonferroni correction as well. A full representation of all of our data and the corresponding p -values can be found in the [supplementary material](#).

HEART RESULTS

Heart rate metrics, as recommended by the most recent overview of heart rate variability metrics and norms (Shaffer and Ginsberg, 2017), were also compared to list type, segment number, and memory scores. We computed the standard deviation and mean for the RR intervals of each subject as well as the following four short-term heart rate variability metrics: pNN50, SD1, SD2, and SDNN (Shaffer and Ginsberg, 2017). Together, these time-domain measurements were also investigated in relation to image regimes and memory. We also looked at how these variables changed over the course of the study within a subject.

Heart results: Heart rate metrics and image regimes

We found significant differences in heart rate metrics when comparing findings between subjects exposed to the pure vs mixed image regimes. These results are similar to our findings in the brain with respect to fractal dimension. Specifically, we found greater heart rate variability in subjects who viewed the mixed image regime compared to subjects who viewed the pure image regime, similar to our findings in EEG. For example, in looking at the overall spread in RR intervals, we found that the standard deviation of the RR intervals was higher during the mixed image regime compared to the pure image regime. The standard deviation (SD) of the RR intervals for mixed image regime subjects is $SD = 90.60$ ms and that of the pure image regime subjects is $SD = 63.89$ ms ($p = 0.056$). The ratio of the standard deviation of RR intervals to the mean RR intervals (SDM) was also higher during the mixed list ($SDM = 0.110$ ms) compared to the pure list ($SDM = 0.078$ ms,

$p = 0.048$). This suggests a higher degree of variability in subjects' RR intervals during the mixed list exposure when compared to the pure list. The scaling of variability based on image regime (i.e., increased variability in response to the more variable mixed image regime) is consistent with our findings in the brain as well.

For the pure vs mixed image regime comparison, we found that pNN50 was statistically significant for segment 7 [pNN50(mixed) = 0.258 vs pNN50(pure) = 0.164, $p = 0.048$]. This result shows that during this segment, pNN50 was higher for the mixed group compared to the pure group. Segment 7 corresponds to the neutral segment for the pure regime and is the only neutral segment sandwiched between two negative segment types. This finding implies that the neutral image regime brought out a low heart rate variability response in subjects, whereas the categorical and negative image regimes inspired variability similar to the mixed list that included all image types. This suggests that neutral image regimes could provide a baseline heart metric of dynamicity in subjects, and this baseline could be used to compare the agility of subjects' responses to other regimes (i.e., a mixed regime) in response to externally applied stimuli. This is consistent with our findings in EEG, where the neutral image regime also had the lowest, baseline FD in comparison to the mixed image regime (Fig. 3).

SDNN also showed significance for the first neutral segment (segment 3) to which the subject was exposed. This result, consistent with our other results, showed that for the mixed group, $SDNN = 96.079$ ms, whereas for the pure list, $SDNN = 48.178$ ms ($p = 0.026$). Though not shown in the other neutral segments, this finding in one neutral segment supports our hypothesis that variability in EKG is present when stimulating beyond the neutral palette. It follows that the neutral segments of the pure image regime may be used as a baseline metric for interpreting deviations away from the baseline as an indicator of resiliency in participants.

Findings in SD1 are similar to our findings in the heart rate metrics above. SD1 conveys the variance of the $y = mx$ line of the Poincaré plot, as discussed in Shaffer and Ginsberg (2017). SD1 is a measure of short-term variability; generally, a higher SD1 is indicative of greater heart rate variability. This is related to the idea that the variable nature of signals coming from physiological systems allows organisms to respond with resilience and adaptability in various quick-response situations. In our study, findings in SD1 mirror previously outlined heart rate metrics to give an insight into subjects' heart rate variability. When comparing the pure vs mixed image regimes, SD1 showed significance in the first neutral segment (segment 3), with $SD1 = 79.59$ ms for the mixed list and $SD1 = 29.04$ ms for the pure list ($p = 0.03$). The higher heart rate variability is correlated with the mixed regime once again for

TABLE III. HRV parameter values for the pure vs mixed image regimes.

HRV parameter	Mixed (M; SE) (ms)	Pure (M; SE) (ms)	p-value
SDNN	90.57; 11.81	63.87; 6.83	0.056
pNN50	.255; .035 (%)	0.181; 0.027 (%)	0.097
SD1	67.83; 12.24	39.13; 7.33	0.05
SD2	1128.63; 27.65	1164.36; 41.59	0.477

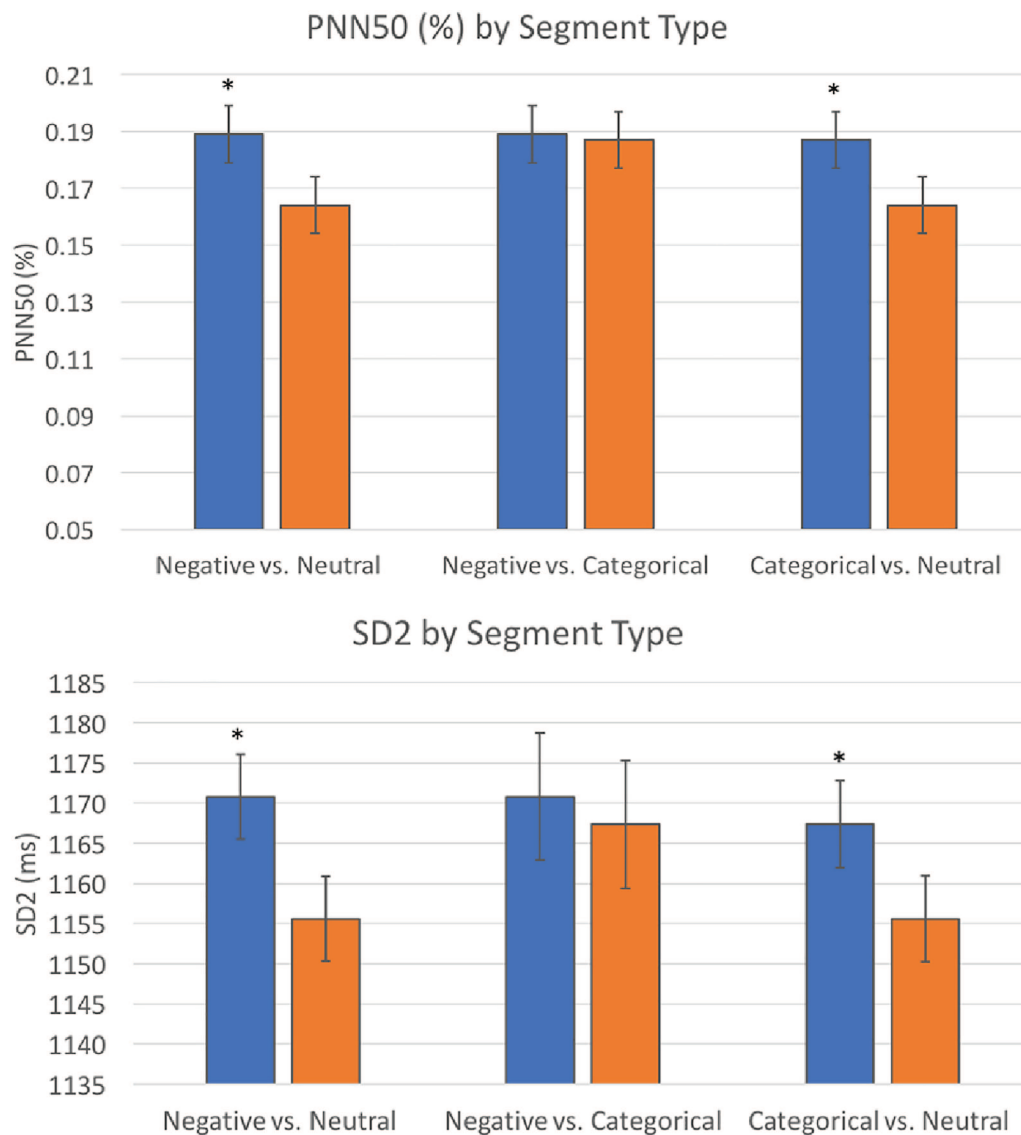


FIG. 7. pNN50 and SD2 for the pure image regime only subjects. This shows significance (denoted by *) within subject for different segment types. Specifically, we compare the heart rate metric of the subject from their negative image segments to their neutral image segments, their negative image segments to their categorical image segments, and their categorical image segments to their neutral image segments. Our study shows significant differences between neutral compared to both negative and categorical.

TABLE IV. A summary of the HRV parameters for the pure image regime comparing the negative, neutral, and categorical image types. p-values that are not significant are labeled as "n.s."

HRV parameter	¹ Negative	² Neutral	³ Categorical	⁽¹⁻²⁾ p-value	⁽²⁻³⁾ p-value
SDNN (ms)	59.67	59.26	64.92	n.s.	n.s.
pNN50 (%)	0.189	0.164	0.187	0.022	0.007
SD1 (ms)	34.34	36.22	40.32	n.s.	n.s.
SD2 (ms)	1170.79	1155.59	1167.35	0.007	0.037

the SD1 parameter. When we look at all the segments averaged, we also find that SD1 is higher for the mixed list (SD1 = 67.83 ms) than for the pure list (SD1 = 39.19 ms, $p = 0.050$). This reinforces the findings above and provides another avenue to see that variability is heightened by the dynamicity of the mixed image regime, which may be important for clinically assessing heart signals based on environmental or external stimuli.

The final heart rate metric we will present in this paper is SD2. SD2 is a measure of the variance on $y = mx + b$ ($b = \text{RR interval average}$) of the Poincaré plot (Shaffer and Ginsberg, 2017). Higher SD2 variance indicates higher heart rate variability (HRV) (Shaffer and Ginsberg, 2017). However, SD2 did not illustrate any significance based on segment number or on overall average of segments. Out of the four heart rate metrics analyzed, this is the only one that did not display a result for this type of analysis. As a result, pure vs mixed image regimes do not seem to be differentiable with this parameter. A summary of our findings in HRV parameters for the pure vs mixed regime is shown in Table III.

We also looked at patterns in HRV for only subjects assigned the pure image regime. The goal was to determine differences between image types (i.e., negative, neutral, or categorical) within a subject. SD2 and pNN50 showed significance within subjects based on the type of images they viewed. These two metrics were investigated in subjects exposed to pure lists only ($n = 31$). Specifically, we compared each subject's heart rate metric during one image type segment (i.e., neutral) to the same subject's results during another image type segment (i.e., negative). In all cases of intra-subject variability, we found that the corresponding heart rate metric was higher during either the negative or the categorical segments when compared to the neutral segments within subjects (Fig. 7). This larger degree of variability based on image type suggests that visual arousal is associated with heightened heart rate variability. After all, negative and categorical images promote relatedness, while negative images also promote arousal and valence (Table II). Furthermore, the neutral segments seem to function as a baseline when compared to more arousing and related images. Categorical compared to negative images did not have distinguishing differences in heart rate variability, suggesting that both have induced the same level of arousal (activation) from a cardiac perspective. This suggests that neutrality might allow the heart to settle into a baseline state that can serve as a control similar to the results we found in the brain. Therefore, using these types of image sequencing might be able to distinguish between subjects that easily adapt to a more arousing stimulus beyond the neutral state and those whose heart rate metrics do not change based on the external stimulus. Reflection on our cardiac results in the healthy heart reveals that comparison of the pure vs mixed image regimes may provide a safe way to investigate heart rate variability within an unhealthy subject. A summary of our findings in HRV parameters for the pure image regime is presented in Table IV.

Heart results: Heart rate metrics and memory

None of the heart rate metrics showed correlation with memory scores.

Averages for all data were also included in the Heart Rate Metric section to protect from any family wise errors. In addition,

the Bonferroni correction is needed when comparing across segment type. For these data, the negative vs neutral comparison for SD2 and RR interval has a p -value < 0.017 (0.007 and 0.004, respectively). For pNN50, the categorical vs neutral has a p -value of 0.007, satisfying this condition as well.

CONCLUSION

Physiological systems depend on the internal function as well as the ability to react to external, environmental stimuli for adaptation and survival. For example, the human heart beats upon activation by an autonomous pacemaker in the heart while simultaneously being affected by numerous neural feedback pathways. These factors work together to produce a normal heart rate consisting of complex fluctuations that occur both naturally and in response to environmental factors (Glass, 2001). Variability has been attributed to overall heart health; healthy subjects often display short-term variations in time intervals between beats and a higher degree of cardiac chaos (Poon and Merrill, 1997). Our research looked at the response of the brain and heart to external image regimes to get a glimpse into how minimal interfacing may set up patterns that could be suggestive of health and fitness (i.e., responsiveness to external stimuli or the propensity for better memory recall).

Our study was conducted in a pool of healthy subjects with no heart or brain abnormalities, and our findings suggest that voltage patterns in subjects may be related to visual stimulation and recall capabilities. These findings show that different image regimes may influence the voltage pattern in the brain and heart. The mixed image regime, which implements a constant switching between neutral, categorical, and negative images, arouses more complex and variable signals in the brain and heart when compared to the pure image regime, which has a fixed set of images for the subject to view. This suggests that an external, variable image regime can evoke a physiological response in both the brain and heart, possibly as an evolutionary response of the body to be more responsive to the unpredictable and varying nature of our environment. Furthermore, we found a correlation between better memory recall and higher fractal dimension but no correlation between better memory recall and greater heart rate variability. This second result suggests that attentiveness may be correlated with more agility in the brain but does not elicit a distinct response in the heart. This may suggest that attentiveness does not demand or need flexible cardiac responsiveness (possibly due to habituation). Taken together with our previous findings, this reinforces our hypothesis that the physiological response of the brain and heart can adjust accordingly to their external environment.

Our results also show that the fractal dimension in EEG scales with the complexity of the external image regime. For example, for the pure vs mixed image regime, the biggest difference in complexity by construction of the experiment is between the mixed regime (most arousing) and the neutral regime (least arousing). The image regimes get closer in their complexity as the pure image regime is tuned from neutral, through categorical and then negative, with the negative images being the closest in complexity to the mixed image regime out of the three image types. The response in EEG as expressed via the fractal dimension mirrors the tuning in complexity—we find the biggest differences between the mixed image

regime when compared to the neutral image regime and this difference starts to fade when comparing mixed and categorical image regimes and then fades even more when comparing mixed and negative image regimes. Likewise, the variability in the heart tracks in the same fashion, with the most complex external image regime (i.e., the mixed image regime) illustrating the most variability in the heart when compared to the pure neutral image regime. Our results suggest that in the heart and brain, a dynamic switching in physiological response occurs to mirror the external trigger. Other authors have hypothesized that these shift in fractal behavior in EEG, for example, are a necessity for survival to switch flexibly from one state to another when triggered. Some authors suggest a theory called the “complexity matching effect” (Allegrini *et al.*, 2006 and West *et al.*, 2008), where the complexity of the external triggers gives rise to the fractal behavior in EEG. Many physiological systems such as the heart also exhibit this type of behavior as a way to be an agile and flexible in response to the stresses of the environment. Some scientists have hypothesized that if nature has fractal features, the body must also have fractal features as a system that has to continually respond to it (Werner, 2010 and Chiavlo, 2010).

Adapting techniques from physics to dynamical systems provides a new lens through which we can understand how neurological and cardiac processes behave. Although our work needs to be scaled to a clinical environment, since pure and mixed image regimes are feasible to mimic in a clinical setting, this method of stimulation may uncover details of how certain pathologies present in the brain and the heart. Based on the simplicity of the calculations and the accessibility of computational techniques, our methods of analysis may provide insight to inform the modification of clinical therapies and to influence patient treatment and care. Furthermore, this paper illustrates the ubiquity of techniques from physics in pursuit of understanding the physical world.

SUPPLEMENTARY MATERIAL

See the [supplementary material](#) for the complete set of all results presented in this paper.

ACKNOWLEDGMENTS

The authors would like to thank Dr. Matt Cathey for his support and review of our statistical analysis. The authors would also like to thank Timothy Phillips and Catherine (Catie) Cronister for help with data cleaning.

DATA AVAILABILITY

The data that support the findings of this study are available from the corresponding author upon reasonable request.

REFERENCES

- Allegrini, P., Bologna, M., Grigolini, P., and West, B. J., “Response of complex systems to complex perturbations: The complexity matching effect,” [arXiv:cond-mat/0612303v1](#) (2006).
- Arsac, L. M. and Deschodt-Arsac, V., “Detrended fluctuation analysis in a simple spreadsheet as a tool for teaching fractal physiology,” *Adv. Physiol. Educ.* **42**, 493–499 (2018).

- Barnacle, G. E., Tsivilis, D., Schaefer, A., and Talmi, D., “Local context influences memory for emotional stimuli but not electrophysiological markers of emotion-dependent attention,” *Psychophysiology* **55**, 1–14 (2018).
- Beck, A. T., Ward, C. H., Mendelson, M., Mock, J., and Erbaugh, J., “An inventory for measuring depression,” *Arch. Gen. Psychiatry* **4**, 561–571 (1961).
- Beck, A. T., Epstein, N., Brown, G., and Steer, R. A., “An inventory for measuring clinical anxiety: Psychometric properties,” *J. Consult. Clin. Psychol.* **56**, 893–897 (1988).
- Captur, G., Karperien, A. L., Hughes, A. D., Francis, D. P., and Moon, J. C., “The fractal heart—Embracing mathematics in the cardiology clinic,” *Nat. Rev. Cardiol.* **14**, 56–64 (2017).
- Chiavlo, D. R., “Emergent complex neural dynamics,” *Nat. Phys.* **6**, 744–750 (2010).
- Dan-Glauser, E. S. and Scherer, K. R., “The Geneva affective picture database (GAPED): A new 730-picture database focusing on valence and normative significance,” *Behav. Res. Methods* **43**, 468–477 (2011).
- Delignieres, D., Ramdani, S., Lemoine, L., Torre, K., Fortes, M., and Ninot, G., “Fractal analyses for ‘short’ time series: A re-assessment of classical methods,” *J. Math. Psychol.* **50**, 525–544 (2006).
- Faes, L., Nollo, G., Jurysta, F., and Marinazzo, D., “Information dynamics of brain-heart physiological networks during sleep,” *New J. Phys.* **16**, 105005 (2014).
- Glass, L., “Synchronization and rhythmic processes in physiology,” *Nature* **410**, 277–284 (2001).
- Goldberger, A. L. and West, B. J., “Fractals in physiology and medicine,” *Yale J. Biol. Med.* **60**, 421–435 (1987).
- Golinska, A. K., “Detrended fluctuation analysis (DFA) in biomedical signal processing: Selected examples,” *Stud. Logic Grammar Rhetoric* **29**, 107–115 (2012).
- Higuchi, T., “Approach to an irregular time series on the basis of the fractal theory,” *Physica D* **31**, 277–283 (1988).
- Ivanov, P. C., Liu, K. K. L., Bartsch, R. P., “Focus on the emerging new fields of network physiology and network medicine,” *New J. Phys.* **18**, 100201 (2016).
- Iyengar, N., Peng, C.-K., Morin, R., Goldberger, A. L., and Lipsitz, L. A., “Age-related alterations in the fractal scaling of cardiac interbeat interval dynamics,” *Am. J. Physiol.* **271**, R1078–R1084 (1996).
- Katz, M., “Fractals and the analysis of waveforms,” *Comput. Biol. Med.* **18**(3), 145 (1988).
- Kensinger, E. A., “Remembering the details: Effects of emotion,” *Emotion Rev.* **1**, 99–113 (2009).
- Kesic, S. and Spasic, S., “Application of Higuchi’s fractal dimensions from basic to clinical neurophysiology: A review,” *Comput. Methods Programs Biomed.* **133**, 55–70 (2016).
- Lang, P. J., Bradley, M. M., and Cuthbert, B. N., *International Affective Picture System (IAPS): Technical Manual and Affective Ratings* (NIMH Center for the Study of Emotion and Attention, 1999).
- Mather, M. and Sutherland, M. R., “Arousal-biased competition in perception and memory,” *Perspect. Psychol. Sci.* **6**, 114–133 (2011).
- Nayyeri, P., “Analyzing electrocardiography (ECG) signal using fractal method,” *Int. J. Curr. Eng. Technol.* **7**, 498–505 (2017).
- Peng, C. K., Havlin, S., Stanley, H. E., and Goldberger, A. L., “Quantification of scaling exponents and crossover phenomena in nonstationary heartbeat time series,” *Chaos* **5**, 82–87 (1995).
- Pincus, S. M. and Goldberger, A. L., “Physiological time-series analysis: What does regularity quantify?,” *Am. J. Physiol.* **266**, H1643–H1656 (1994).
- Piper, D., Schiecke, K., Pester, B., Benninger, F., Feucht, M., and Witte, H., “Time-variant coherence between heart rate variability and EEG activity in epileptic patients: An advanced coupling analysis between physiological networks,” *New J. Phys.* **16**, 11 (2014).
- Piskorski, J. and Guzik, P., “Geometry of the Poincare plot of RR intervals and its asymmetry in healthy adults,” *Physiol. Meas.* **28**, 287–300 (2007).
- Poon, C.-S. and Merrill, C. K., “Decrease of cardiac chaos in congestive heart failure,” *Nature* **389**, 492–495 (1997).
- Riley, M. A., Bonnette, S., Kuznetsov, N., Wallot, S., and Gao, J., “A tutorial introduction to adaptive fractal analysis,” *Front. Physiol.* **3**, 1–10 (2012).

- Schmidt, S. R. and Saari, B., "The emotional memory effect: Differential processing or item distinctiveness?," *Mem. Cognit.* **35**, 1905–1916 (2007).
- "Sgolay," MathWorks, Savitzky-Golay filter design—MATLAB, see <https://www.mathworks.com/help/signal/ref/sgolay.html>.
- Shaffer, F. and Ginsberg, J. P., "An overview of heart rate variability metrics and norms," *Front. Public Health* **5**, 1–17 (2017).
- Stam, C. J., "Nonlinear dynamical analysis of EEG and MEG: Review of an emerging field," *Clin. Neurophysiol.* **116**, 226–2301 (2005).
- Talmi, D. and Moscovitch, M., "Can semantic relatedness explain the enhancement of memory for emotional words?," *Mem. Cognit.* **32**, 742–751 (2004).
- Talmi, D., Luk, B. T. C., McGarry, L. M., and Moscovitch, M., "The contribution of relatedness and distinctiveness to emotionally-enhanced memory," *J. Mem. Lang.* **56**, 555–574 (2007).
- Talmi, D. and McGarry, L. M., "Accounting for immediate emotional memory enhancement," *J. Mem. Lang.* **66**, 93–108 (2012).
- Talmi, D., "Enhanced emotional memory: Cognitive and neural mechanisms," *Curr. Dir. Psychol. Sci.* **22**, 430–436 (2013).
- Watts, S., Buratto, L. G., Brotherhood, E. V., Barnacle, G. E., and Schaefer, A., "The neural fate of neutral information in emotion-enhanced memory," *Psychophysiology* **51**, 673–684 (2014).
- Werner, G., "Fractals in the nervous system: Conceptual implications for theoretical neuroscience," *Front. Physiol.* **1**, 1–28 (2010).
- Wessa, M., Kanske, P., Neumeister, P., Bode, K., Heissler, J., and Schonfelder, S., "Emopics: Subjective and psychophysiological evaluations of new visual material for clinical-bio-psychological research," *J. Clin. Psychol. Psychother.* **1**, 77 (2010).
- West, B. J., Geneston, E. L., and Grigolini, P., "Maximizing information exchange between complex networks," *Phys. Rep.* **468**, 1–99 (2008).
- Wright, J. J., Kydd, R. R., and Liley, D. T. J., "EEG models, chaotic and linear," *Psychology* **4**, eeg-chaos.l.wright (1993).